Proceedings of ISFOG 2025
5TH INTERNATIONAL SYMPOSIUM ON
FRONTIERS IN OFFSHORE GEOTECHNICS
Nantes, France | June 9-13 2025

ISBN 978-2-85782-758-0

Analytical base shear reaction curves for predicting monopile response in undrained clay

C. Walker
University of Bristol, Bristol, UK

G. Mylonakis
University of Bristol, Bristol, UK,
and Khalifa University, Abu Dhabi, UAE

D. Karamitros
University of Bristol, Bristol, UK

J. J. Crispin, A. H. Bateman*
University of Southampton, Southampton, UK

**a.bateman@soton.ac.uk (corresponding author)*

ABSTRACT: Incorporating soil reaction curves at the monopile tip when calculating the response at the monopile head reduces overprediction of deformations when compared with solely employing traditional *p-y* models. This is particularly important for squat monopile foundations that are often used for offshore wind turbines. However, published soil reaction curves at the pile tip are limited in number and are the subject of far less research than the commonly employed *p-y* curves. In this work, closed-form expressions for the shear response at the pile tip are developed using a cone model for the soil material under the pile base, combined with a number of simplified non-linear soil constitutive models. The solutions can be used in conjunction with available *p-y* curves to obtain the full displacement response of monopile foundations without the need for time-consuming 3D numerical analyses, which is particularly useful in the early stages of design. The resultant non-linear expressions are compared with available solutions using a two-part similarity approach.

Keywords: Monopiles; Shear base curve; Soil reaction; Cone model; Undrained clay

1 INTRODUCTION

Monopile foundations continue to be the leading solution for supporting Offshore Wind Turbines (OWTs), accounting for 70% of all new and existing OWT foundations deployed by the end of 2022 (Williams and Zhao, 2024). They comprise a single, steel tube with a low slenderness ratio (L/D) on the order of 3 to 6 and are typically employed in water depths of up to 50m, where pile behaviour is governed by wind, wave and current loading (i.e., lateral loading).

Laterally loaded pile design traditionally uses idealised distributed lateral load-displacement springs (*p-y*) along the pile length to imitate the horizontal soil reaction at the pile-soil interface. These springs can be used to incorporate non-linear soil behaviour and have been widely applied in the offshore industry for over 50 years (e.g., McClelland and Focht, 1956; Matlock 1970; Reese and Van Impe 2011). However, *p-y* models tend to overpredict the lateral displacement response, particularly for squat monopile foundations (slenderness ratio $L/D < 10$). Predictions of monopile displacements using *p-y* curves can be improved by considering the distributed moment response (e.g., Bateman, 2025; Bateman et al., 2025a) as well as the horizontal and moment resistance at the pile base. Although the importance of directly incorporating the response of the pile base is well documented (see Jeanjean and Zakeri, 2023), solutions for these soil reaction curves are limited.

The PISA design model (Byrne et al, 2020) incorporates these additional curves. Specifically, this method generates non-linear soil reaction curves at the pile base from field test results that undergo a three-stage calibration using three-dimensional finite element analysis (FEA). However, a reliance on site-specific testing and computationally demanding software deems this method less than ideal for use at early stages of design.

As an alternative, a simple approach was proposed that obtains shear and moment curves at the pile base by assuming the elastic and plastic components are similar in shape to the corresponding parts of a soil

element test (Zhang and Andersen, 2019; Fu et al., 2020). Adopting this approach, elastic and plastic linear transformation factors can be employed to predict the base curves. This method, referred to herein as "two-part similarity", is an extension of the classical similarity approach, introduced by Skempton (1951) for a vertically loaded surface footing that employs a single transformation factor to translate footing settlement to soil strain and vice versa. Lai et al. (2021) also used a similar "two-part" similarity approach to obtain a lumped curve, applied at the point of rotation, that accounts for both base curves and the remaining shaft resistance below this point. However, while classical similarity has frequently been used to derive *p-y* curves, this simpler method has not been investigated for the base soil reaction curves. In addition, limited validation of the "two-part" method has been undertaken.

A possible alternative to this existing approach is the cone model (Wolf and Deeks 2004), which has been widely used to determine the dynamic stiffnesses and damping of foundations. This allows the problem to be considered in closed form, even when introducing soil non-linearity. Bateman et al. (2025b) proposed a similar solution for vertically loaded surface foundations in non-linear soils.

Motivated by the lack of solutions for the base response of monopile foundations and the lack of validation of the existing "two-part" similarity approach, this paper presents an analytical approach for deriving the "base shear" curves using a cone model. This method aims to provide reasonable estimations at the early stages of design, allowing for quick feasibility predictions. Moreover, this paper will compare the solutions to those predicted using the "two-part" similarity approach of Zhang and Andersen (2019). An early version of this work can be found in Walker (2024).

2 CONE MODEL

The cone model, illustrated in Figure 1, proposes that shear stresses applied at the pile base (of radius r_0 and area A_0) would generate corresponding shear stresses on horizontal planes in the underlying soil. At depth z, the area bounded by the semi-infinite truncated cone is defined with a radius r_z and an area A_z. The shear stresses are assumed to attenuate with depth, such that the horizontal force remains constant (but acts over a larger area). This can be expressed by Eq. 1.

$$S_z = S_0 \frac{A_0}{A_z} \tag{1}$$

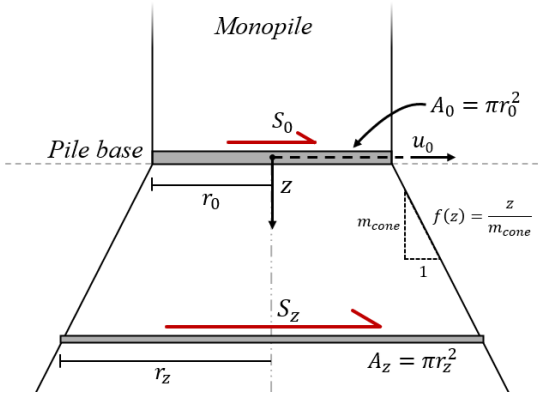

Figure 1: Application of the cone model to obtain the base shear curve for a laterally loaded monopile tip.

where S_0 and S_z are the shear stresses acting at the pile tip and at depth z beneath the pile tip, respectively.

The cone model relies on a number of assumptions:

1. The monopile is assumed to develop a soil plug, with a perfect shearing interface at the pile base, which can instead be represented by a rough, rigid, two-dimensional disk.
2. The soil is assumed to be homogenous and isotropic, and material outside of the semi-infinite cone is neglected.
3. Pile installation effects are ignored.
4. Plane cross-sections of the cone remain plane.
5. The cone opening angle is m_{cone} (discussed below).
6. Loading is static and unidirectional.

In conflict with point 2, variations of the strength and stiffness of the clay with depth are common. This variation could be incorporated in the integral below by allowing the strength and stiffness to be functions of depth z; however, this additional complexity lies beyond the scope of this work.

The lateral displacement at the pile base, u_0, can be calculated by integrating shear strain, γ, in the soil with respect to depth beneath the pile tip, z:

$$u_0 = \int_0^\infty \gamma \, dz \tag{2}$$

The shear strain in the soil can be calculated from the corresponding shear stress, τ, using a pertinent soil model in flexibility form ($\gamma(\tau)$ relationship). Simple elastic and non-linear expressions are discussed below. The shear stresses in the soil can be assumed equal to those developed in the cone itself:

$$\tau = S_z = S_0 \frac{A_0}{A_z} \tag{3}$$

The area of the cone at depth z can be given by:

$$A_z = \pi\, r_z^2 = \pi\, r_0^2 \left(1 + \frac{z}{r_0\, m_{cone}}\right)^2 \qquad (4)$$

where r_z is the radius of the circular area enclosed by the cone at depth z.

Substituting Eq. 4 into Eq. 3 and selecting a suitable soil constitutive model, in flexibility form $\gamma = f(\tau)$, enables a function of γ in terms of z to be established. This function can be input into Eq. 2 to obtain the lateral displacement of the pile tip due to a corresponding applied load (a base shear curve). This paper considers three soil constitutive models: linear-elastic, power-law and hyperbolic. The first two models require a manual cut-off at the soil undrained shear strength, s_u, while the hyperbolic model asymptotically approaches this value.

3 LINEAR-ELASTIC SOIL

The simplest $\gamma(\tau)$ relationship is the linear-elastic model, typically most applicable at low values of shear stress when the soil can be assumed to be within its elastic range. This can be given by:

$$\gamma = \frac{\tau}{G} \qquad (5)$$

where G is the shear modulus.

This is plotted in Figure 2a, normalised by the undrained shear strength, s_u. Substituting Eqs. 3 and 4 into this model and integrating with respect to depth (Eq. 2), the following expression of an elastic base shear curve is obtained:

$$S_0 = \frac{2G}{m_{cone}}\left(\frac{u_0}{D}\right) \qquad (6)$$

By matching the above horizontal static-stiffness coefficients with the rigorous elastostatic solution by Mindlin (1949), Wolf and Deeks (2004) suggest the opening angle of the cone, m_{cone}, can be given:

$$m_{cone} = \frac{z}{r_z - r_0} = \frac{\pi}{8}(2 - \nu) \approx 0.6 \qquad (7)$$

where ν is the Poisson's ratio of the soil. This curve is plotted in Figure 2b, normalised against the ultimate lateral capacity of the pile tip:

$$S_{0,ult} = s_u \qquad (8)$$

3.1 Comparison with existing solutions

Existing solutions for the base shear curves are derived using a "two-part" similarity approach (Zhang and Andersen, 2019; Fu et al. 2020). This method assumes the elastic and the plastic components of the base shear curve are similar in shape to the corresponding portion of the soil element test (often idealised using a soil constitutive model). Therefore, elastic and plastic linear transformation factors can be employed to predict the base shear curve, written as:

$$\frac{u_0}{D} = \xi_e \gamma_e + \xi_p \gamma_p \qquad (9)$$

where ξ_e and ξ_p are the linear transformation factors that are applied to the elastic strain, γ_e and plastic strain, γ_p, respectively.

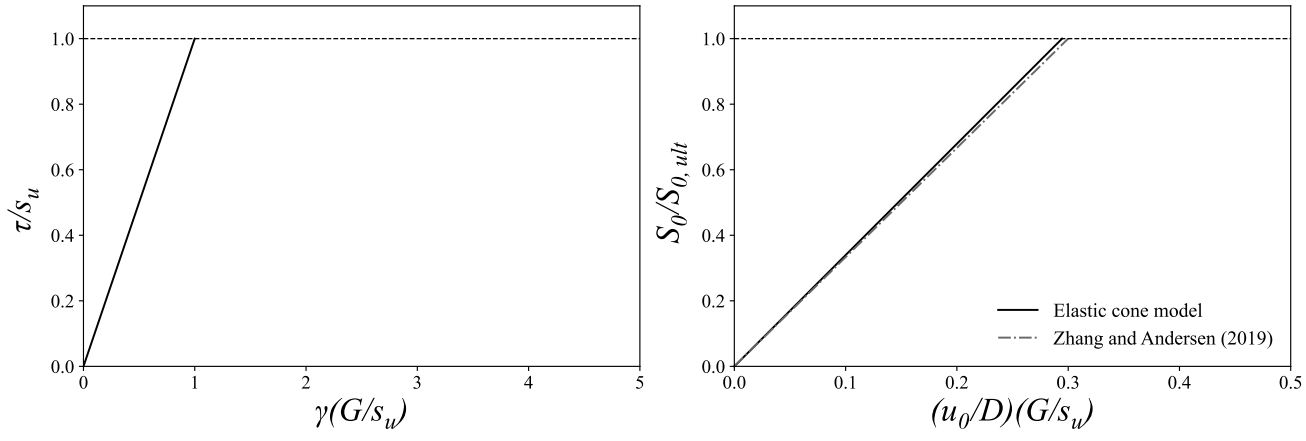

(a) (b)

Figure 2: Linear-elastic model: (a) Soil constitutive behaviour and (b) the corresponding shear base curve

From a finite-element analysis of a surface footing on uniform clay, Zhang and Andersen (2019) calculate $\xi_e = 0.3$ and $\xi_p = 0.12$.

Using the cone model and comparing Eq. 6 and Eq. 5 enables the ξ_e from this work to be calculated. This yields:

$$\frac{u_0}{D} = \frac{m_{cone}}{2}\,\gamma \tag{10a}$$

$$\xi_e = \frac{m_{cone}}{2} \approx 0.3 \tag{10b}$$

This suggests that ξ_e is dependent on the selected cone opening angle, which makes sense as the specific angle is, itself, a calibrated stiffness parameter. When $m_{cone} \approx 0.6$ (see Eq. 7; Wolf and Deeks, 2004), ξ_e matches the value calculated by Zhang and Andersen (2019).

4 NON-LINEAR SOIL

It is well-known that soil is an inherently non-linear material. The cone model approach in this paper enables the use of any simplified non-linear soil constitutive model, that can be expressed in flexibility form, to obtain non-linear base shear curves.

4.1 Power-law model

The power-law requires two additional parameters, γ_{50}, which represents the shear strain exhibited when shear stress reaches 50% of the undrained shear strength, and a power exponent, b (Vardanega and Bolton 2011):

$$\gamma = \gamma_{50}\left(\frac{2\tau}{s_u}\right)^{\frac{1}{b}} \tag{11}$$

This model is plotted in Figure 3a ($b = 0.6$; Vardanega and Bolton, 2011). Vardanega and Bolton (2011) suggest this model is most applicable between $0.2 < \tau/s_u < 0.8$. Using Eqs. 2, 3, 4 and 11, the base shear curve for the power-law soil constitutive model can be calculated as:

$$\frac{u_0}{D} = \frac{\gamma_{50}\, b\, m_{cone}}{2(2-b)}\left(\frac{2S_0}{s_u}\right)^{\frac{1}{b}} \tag{12}$$

Note that the initial stiffness of the power-law model is infinite, hence there is only plastic strain generated. Therefore, applying Eq. 9 (Zhang and Andersen, 2019) is the same as scaling Eq. 11 by ξ_p ($\xi_p = 0.12$ from Zhang and Andersen, 2019). An equivalent ξ_p can be calculated for the power-law model:

$$\xi_p = \frac{b\, m_{cone}}{2(2-b)} \tag{13}$$

Remarkably, this is equal to 0.13 when $m_{cone} = 0.6$ (Eq. 7; Wolf and Deeks, 2004) and $b = 0.6$, given by Vardanega and Bolton (2011) as the average b fitted to a database of clays and silts. The base shear curve calculated from the cone model is compared to that scaled from Zhang and Andersen (2019) in Figure 3b.

4.2 Hyperbolic model

The hyperbolic model produces a stress-strain profile with initial stiffness G and asymptotes towards the undrained shear strength, s_u, as shown in Figure 4a and described by Kondner (1963):

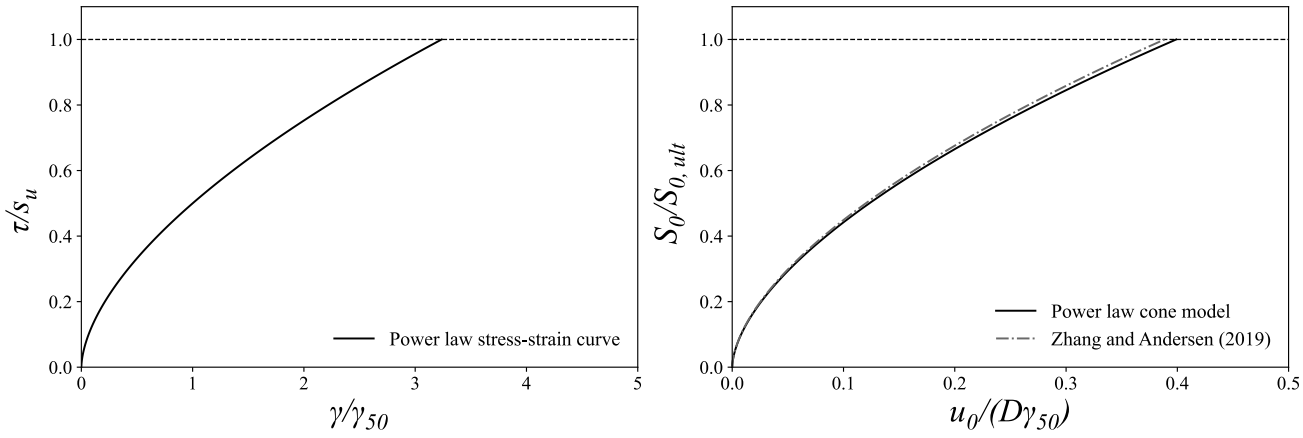

(a) (b)

Figure 3: Power-law model: (a) Soil constitutive behaviour and (b) the corresponding shear base curve ($b = 0.6$; Vardanega and Bolton 2011)

$$\gamma = \left(\frac{s_u}{G}\right)\frac{1}{\frac{s_u}{\tau} - 1} \quad (14)$$

Following a similar procedure to the linear-elastic model, the base shear curve obtained from the cone model is given by:

$$\frac{u_0}{D} = \frac{m_{cone}\sqrt{S_0/s_u}}{4}\left(\frac{s_u}{G}\right)\ln\left(\frac{1+\sqrt{S_0/s_u}}{1-\sqrt{S_0/s_u}}\right) \quad (15)$$

The above equation has been plotted in Figure 4b alongside the linear-elastic model solution derived in Eq. 6. In addition, the base shear curve that is obtained by scaling the hyperbolic soil constitutive model is included for comparison, derived using Eq. 9 (Zhang and Andersen, 2019). As expected, the elastic portion of the curve is a good match to Zhang and Andersen (2019). However, the base shear curve deviates at higher loading, indicating the "two-part" similarity method under-estimates the stiffness of the base shear curve at higher loads compared to the cone model.

5 CONCLUSIONS

Incorporating the horizontal resistance of the pile tip (base shear curve) is important when calculating monopile displacements. Simplified solutions to these curves are advantageous at the early stages of design, allowing for quick feasibility predictions. However, existing methods to obtain these soil reaction curves using simplified approaches are limited to a "two-part" similarity method, with limited validation.

Motivated by this lack of knowledge, this paper has presented an analytical approach for deriving the base shear curve. This employs a cone model in which the shear stresses are assumed to attenuate with depth, such that the horizontal force remains constant (Figure 1). This approach enables simplified non-linear soil constitutive models in flexibility form to be employed, yielding closed-form solutions for the base shear curve. To this end:

- A linear-elastic soil constitutive model is used to derive a base shear curve given in closed-form in Eq. 6.
- This elastic solution is used to derive a closed-form solution for ξ_e, given by Eq.10, which validates the ξ_e $(= 0.3)$ from Zhang and Andersen (2019), shown in Figure 2.
- A power-law and a hyperbolic soil constitutive model are employed in the cone model approach to derive closed-form base shear curves in Eqs. 12 and 15.
- The power-law solution is used to derive a closed-form solution for ξ_p, given by Eq. 13. This solution is within 5% of that obtained using FEA by Zhang and Andersen (2019), shown in Figure 3.
- The hyperbolic solution is compared with that obtained by Zhang and Andersen (2019) in Figure 4. The two methods provide very similar results at low stresses and deviate at higher stresses. Notably, the cone model yields stiffer estimates.
- The analytical solutions indicate that at 50% of ultimate capacity, the normalised horizontal displacement of the tip lies in the range $u_0/D = 0.15\text{-}0.25\ s_u/G$. Since s_u/G is about 10^{-3} to 10^{-2}, this displacement is approximately 1.5×10^{-4} to 2.5×10^{-3} times the monopile diameter.

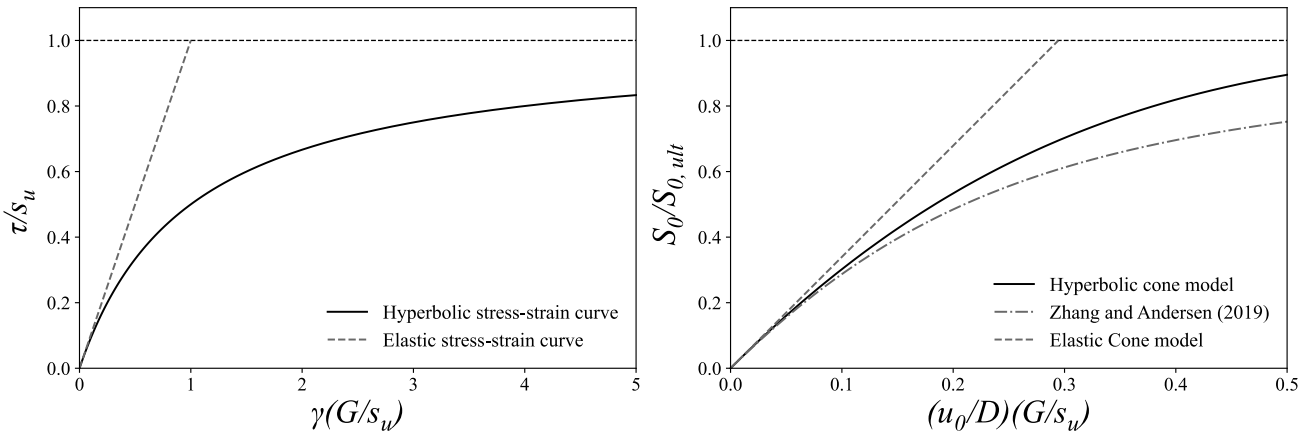

(a) (b)

Figure 4: Hyperbolic model: (a) Soil constitutive behaviour and (b) the corresponding shear base curve

- Given a rigid pile, of length L, rotating about a depth of $2L/3$, if an ultimate capacity criterion of $0.1D$ displacement is applied at the pile head, a $0.05D$ lateral displacement is observed at the pile tip. Given s_u/G of about 10^{-3} to 10^{-2}, these curves are essentially fully mobilised, highlighting the importance of incorporating their response.

Validation of these findings, both as a standalone result and in conjunction with other soil reaction curves to predict the full monopile response, is required before these are employed in design practice. This task can be undertaken through comparison with field tests data or three-dimensional FEA.

AUTHOR CONTRIBUTION STATEMENT

Cameron Walker: Formal analysis, Writing – original draft, Visualisation. **Dimitris Karamitros**: Conceptualisation, Writing – review and editing. **George Mylonakis**: Supervision, Writing – review & editing. **Jamie Crispin**: Conceptualisation, Methodology, Writing - review and editing. **Abigail Bateman**: Formal analysis, Methodology, Supervision, Validation, Writing – original draft, Writing – review and editing.

ACKNOWLEDGEMENTS

Abigail Bateman is supported by the Offshore Renewable Energy Supergen Hub Project (EPSRC grant EP/Y016297/1).

REFERENCES

Bateman, A. H. (2025). *Simplified solutions for the non-linear analysis of axially and laterally loaded piles in clay.* PhD Thesis. Department of Civil Engineering, University of Bristol, Bristol, UK.

Bateman, A.H., Crispin, J.J., and Mylonakis, G. (2025a). Analytical nonlinear '*m-θ*' curves for monopiles in clay. *Journal of Geotechnical and Geoenvironmental Engineering, ASCE*, 151(5), 04025024. https://doi.org/10.1061/JGGEFK.GTENG-12889

Bateman, A. H., Crispin, J. J., Karamitros, D., and Mylonakis, G. (2025b). Similarity based nonlinear settlement predictions of circular surface footings on clay. *Journal of Geotechnical and Geoenvironmental Engineering, ASCE.* https://doi.org/10.1061/JGGEFK.GTENG-12641

Byrne, B.W., Houlsby, G.T., Burd, H.J., et al. (2020). PISA design model for monopiles for offshore wind turbines: application to a marine sand. *Géotechnique*, 70(11): 1030–1047. https://doi.org/10/ghnv93.

Fu, D., Zhang, Y., Aamodt, K.K., Yan, Y. (2020). A multi-spring model for monopile analysis in soft clay. *Marine structures*, 72, 102768. https://doi.org/gn7hz5.

Jeanjean, P. and Zakeri, A. (2023). Efficiencies and challenges in offshore wind foundation design. *9th International Offshore Site Investigation and Geotechnics Conference*, London, UK. https://doi.org/nqqc.

Kondner, R.L. (1963). Hyperbolic Stress-Strain Response: Cohesive Soils. Journal of the Soil Mechanics and Foundations Division, ASCE, 89(1): 115–143. https://doi.org/10/gmfpn2.

Lai, Y., Wang, L., Zhang, Y., Hong, Y. (2021). Site-specific soil reaction model for monopiles in soft clay based on laboratory element stress-strain curves. *Ocean Engineering*, 220, 108437. https://doi.org/10/gj2kj3.

Matlock, H. (1970). Correlations for design of laterally loaded piles in soft clay. Proceedings of the 2nd Offshore Technology Conference, Houston, Texas, USA, 557–588. https://doi.org/cmzcw4.

McClelland, B., and Focht, J. A. (1956). Soil Modulus for Laterally Loaded Piles. Journal of the Soil Mechanics and Foundations Division, ASCE, 82(4), 1081. https://doi.org/10/gmg6rk.

Mindlin, R.D. (1949). Compliance of Elastic Bodies in Contact, Journal of Applied Mechanics, 16(3), 259-268

Reese L.C. and Van Impe, W.F. (2011). Single Piles and Pile Groups under Lateral Loading, CRC Press, London.

Skempton, A. W. (1951). The bearing capacity of clays. *Building Research Congress*, 1, 180–189.

Vardanega, P. J., and Bolton, M. D. (2011). Strength mobilization in clays and silts. Canadian Geotechnical Journal, 48(10), 1485–1503. https://doi.org/ 10/b6wmz5. [corrigendum 49(5): 631].

Walker, C. (2024). *Simplified prediction methods for non-linear offshore monopile base reaction curves in clay.* Undergraduate Research Report No. 2324RP087. Civil Engineering Programme, School of Civil, Aerospace and Design Engineering, University of Bristol, Bristol, UK.

Williams, R. and Zhao, F. (2024). *Global Offshore Wind Report 2024*. Global Wind Energy Council (GWEC), Brussels, Belgium.

Wolf, J.P. and Deeks, A.J. (2004). *Foundation Vibration Analysis: A Strength-of-materials Approach*. 1st Edition. Butterworth-Heinemann.

Zhang, Y. and Andersen, K.H. (2019). Soil reaction curves for monopiles in clay. Marine structures, 65, 94-113. https://doi.org/10/gn7hvp.